Mausam, (1995), 46, 4, 409-422

551.465.11 : 551.513 (267)

A numerical modelling study of the interannual variability in the Indian Ocean

S. K. BEHERA and P. S. SALVEKAR
Indian Institute of Tropical Meteorology, Pune
(Received 9 March 1994, Modified 25 November 1994)

सार — हिन्द महासागर (24° द०-23° उ० और 35° पू०-115° पू०) के ऊपरी भाग में अन्तरवार्षिक परिवर्तिता का अध्ययन करने के लिए एक सरल गुरुत्व न्यूनीकृत पवन/परिचालित महासागर परिसंचरण निदर्श का प्रयोग किया गया है। इस निदर्श में 1977 से 1986 की अवधि के मासिक माध्य पवन प्रतिबल का दबाव के रूप में प्रयोग किया गया है। जब इस निदर्श को दस वर्षों की औसत मासिक माध्य पवन के साथ बलीयित किया गया तब हिन्द महासागर के ऊपरी भाग परिसंचरण के वार्षिक चक्र के अधिकांशत: प्रेक्षित लक्षण इससे उत्पन्न हुए। परिसंचरण लक्षणों और मॉडल के ऊपरी भाग की स्थूलता से द्रोणी के अधिकांश भागों विशेषकर सोमाली धारा, दक्षिणी गोलार्ध वृत्ताकार गति, द्रोणी भूमध्य रेखीय धाराओं और बंगाल की खाड़ी में वृत्ताकार गति (जायर) में पर्याप्त अन्तरवार्षिक परिवर्तिता का पता चलता है। अन्तरवार्षिक परिवर्तिता का अध्ययन करने के लिए 1978 से 1983 तक के छ: (6) क्रमिक वर्ष लिए गए जिसमें 1979 और 1982 के दो खराब मानसून वर्ष भी शामिल हैं। फरवरी के परिसंचरण क्षेत्रों को देखने से पता चलता है कि खराब मानसून वर्षों में भूमध्य रेखीय प्रति धाराएं अपेक्षाकृत अधिक प्रबल हैं जबकि अच्छे मानसून वर्षों में अफ्रीकी तट तक बहने वाली मैडागास्कर के उत्तर की धाराएं अपेक्षाकृत प्रबल पायी गई हैं। खराब मानसून वर्षों में अगस्त माह में दक्षिणी वृत्ताकार गति से दक्षिणाभिमुखी प्रत्यावर्तित प्रवाह दक्षिणी अक्षांश में प्रबल से अधिक प्रबल तक पाया गया है। दक्षिणी वृत्ताकार गति के पूर्व में अन्य भंवर के साथ प्रवाह का परिसंचरण पूर्वाभिमुखी है। दक्षिणी गोलार्द्ध की वृत्ताकार गति (जायर) द्रोणी में व्यातिरेक वर्षों की तुलना में दो क्रमिक सामान्य वर्षों में कम परिवर्तिता का पता चलता है।

ABSTRACT. A simple reduced gravity wind-driven ocean circulation model is used to study the interannual variability in the upper layer of the Indian Ocean (24°S-23°N and 35°E-115°E). The monthly mean wind stress for the period 1977-1986 are used as a forcing in the model. The model reproduces most of the observed features of the annual cycle of the upper layer circulation in the Indian Ocean when was forced with the ten-year average monthly mean wind. The circulation features and the model upper layer thickness show considerable interannual variability in most part of the basin; in particular, the Somali Current, the basin wide southern hemisphere gyre, the Equatorial Currents and the gyres in the Bay of Bengal. Six consecutive years starting from 1978 to 1983 which include two bad monsoon years of 1979 and 1982 are chosen to study the interannual variability. February circulation field shows stronger Equatorial Counter Currents in bad monsoon years, whereas, the currents north of Madagascar flowing up to the African coast are found to be stronger in good monsoon years. The southward return flow from the Southern Gyre in August is strong and more to southern latitudes in the bad monsoon years. The flow circulated eastward to form another eddy east of Southern Gyre. The basin wide gyre of the southern hemisphere (SH) shows less variability in two consecutive normal years than in contrasting years.

Key words — Reduced gravity, Transport, Indian Ocean, Circulation, Interannual variability.

1. Introduction

Following the work of Cox (1970), in the last two decades there have been considerable mathematical modelling work for the Indian Ocean, *e.g.*, Luther *et al.* (1985), Luther & O' Brien (1989), McCreary & Kundu (1988), Das *et al.* (1987) and Jensen (1990). Cox (1970) used a three dimensional oceanic general circulation model with seven levels in vertical direction, whereas, most of the other workers used layer models with assumption of one or more active layers over an infinitely deep motionless layer. These layer models with less vertical resolution and less prognostic equations require relatively small computational resources compared to oceanic general circulation models. These models do not include prognostic thermohaline equations, but due to their computational efficiency they can be used for several numerical experiments to study their sensitivity to various forcings, boundary conditions and geometries. These models can also be modified to include additional physics, *e.g.*, Zebiac and Cane (1987) added a mixed layer of constant depth with thermodynamics on the top of the upper layer and coupled the ocean model to a simple atmosphere model (Gill 1980) to study the ENSO phenomenon.

Luther *et al.* (1985) using a one and half layer model with two different wind forcings simulated realistically the Somali Current and the associated gyre system. Luther & O' Brien (1989) using 23-year mean monthly wind data (Cadet and Diehl 1984) showed the interannual variability in Somali

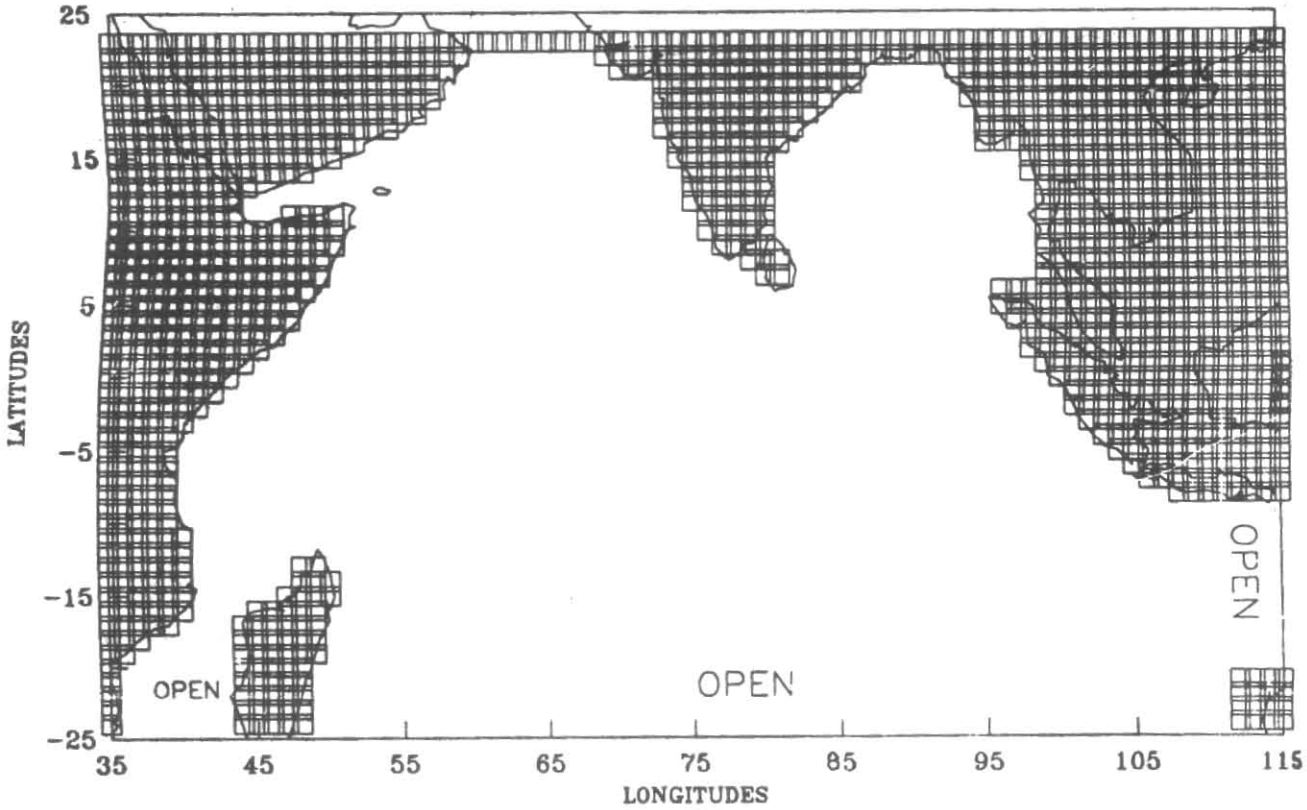

Fig. 1. The model geometry, considered in the present study. Hatched parts are land boundaries

Current and the Indian Ocean. Jensen (1990) simulated the sub-surface circulations besides the surface circulation of the Indian Ocean using a three and half layer model. Dube *et al.* (1990) investigated the relationship between the interannual variability in model fields of central Arabian Sea with the Indian monsoon rainfall.

In the present study, a simple one and half layer reduced gravity transport model is used to study the wind driven ocean circulation of the Indian Ocean and to determine the interannual variability.

2. The model equations

The model used for this study has one active layer, overlying a deep motion less inactive layer, *i.e.,* zero pressure gradient in the lower layer which effectively filters the fast barotropic modes. The model equations are based on vertically integrated shallow water equations over a layer, assuming no vertical shear in horizontal fields.

The model equations in cartesian co-ordinate are;

$$U_t + (UU/H)_x + (UV/H)_y - fV + (g'/2)^* (H^2)_x = A_H \nabla^2(U) + \tau_{xz}/\rho_1 \quad (1)$$

$$V_t + (UV/H)_x + (VV/H)_y + fU + (g'/2)^* (H^2)_y = A_H \nabla^2(V) + \tau_{yz}/\rho_1 \quad (2)$$

$$H_t + U_x + V_y = O \quad (3)$$

Where U and V are zonal and meridional components of vertically integrated upper layer velocity components, f is the Coriolis parameter ($2\Omega\sin\phi$). H is the upper layer thickness, $g' = g(\rho_2 - \rho_1)/\rho_2$ is the reduced gravity. A_H is the horizontal eddy viscosity and (τ_{xz}, τ_{yz}) are the components of the wind stress applied as a body force.

The model equations are solved numerically on a finite difference mesh staggered in space (Arakawa C grid) with a horizontal resolution of ~ 28 km. The equations are integrated over time using leap-frog finite-difference scheme, with a time step of 30 min. An Euler scheme is applied at every 49th step to eliminate errors due to time-splitting inherent in leap-frog scheme. The parameters used in this study are $A_H = 3000$ m^2s^{-1}, $g' = .03$ ms^{-2} and the initial upper layer depth $H_0 = 200$ m.

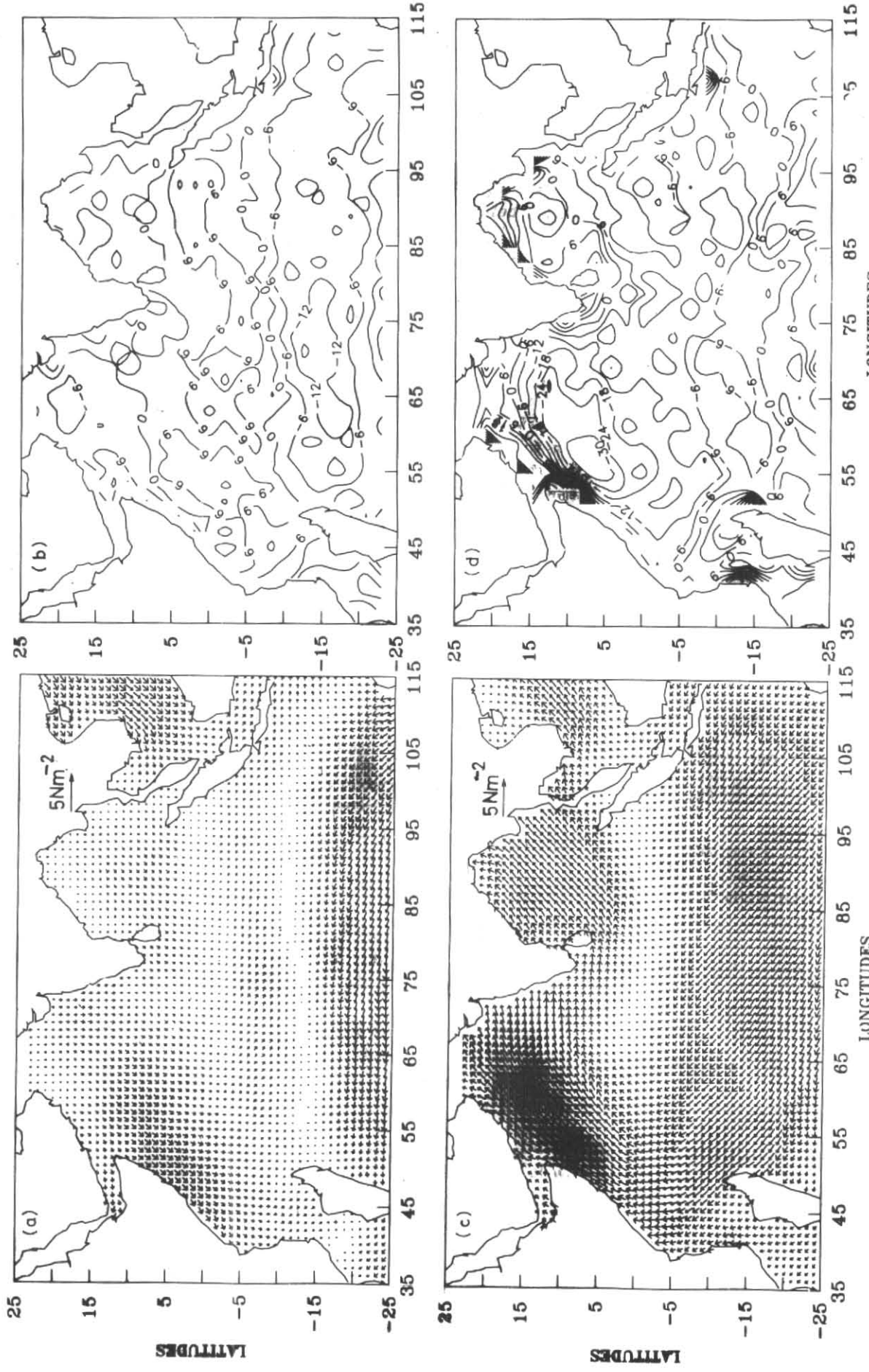

Figs. 2 (a & b). Average wind stress and wind stress curl for February taken from the 10 years mean monthly data. Contour interval for the wind stress curl is $6*10^{-8}$ N m^{-3}

Figs. 2 (c & d). Same as Figs. 2 (a) & (b), but for the month of August

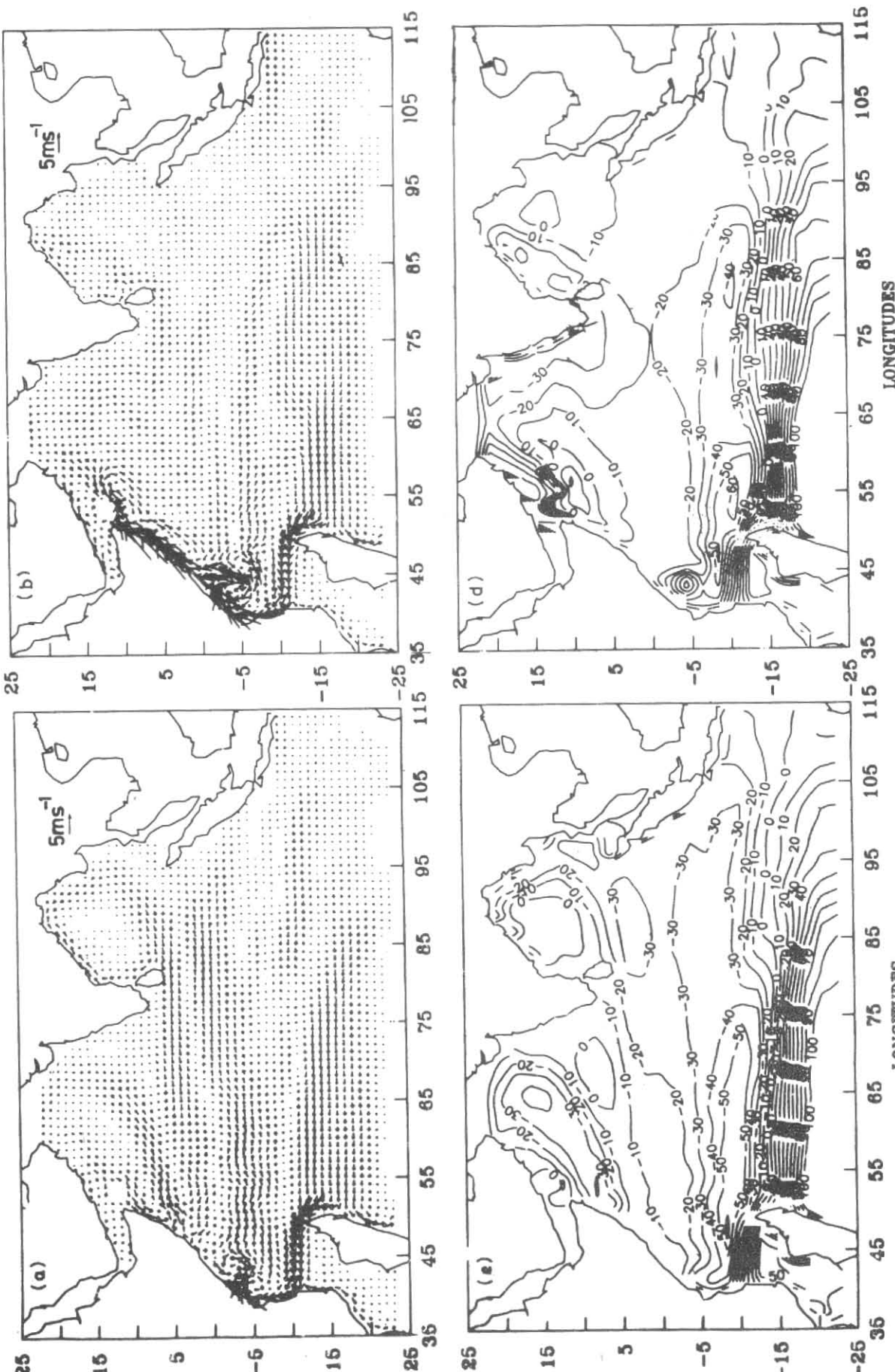

Figs. 3 (a-d) Model fields obtained in the case of the 10-year average wind stress forcing: (a) 16 February circulation. (b) 16 August circulation. (c) 16 February upper layer thickness deviation. (d) same as (c) but for 16 August. Only one arrow is shown at each one degree of latitude and longitude. Arrows representing less than 0.01 ms^{-1} are suppressed. ULT deviation contour interval is 10 m

The model geometry considered in this study is from 35°E to 115°E and from 24°S to 23°N (Fig. 1). Boundary conditions at land boundaries are no slip ($U = V = 0$) and modified radiation boundary condition (Camerlengo and O' Brien 1980, Jensen 1990) is applied at the open boundaries.

2.1. *Model input*

Mean wind pseudo-stress are made available for the poriod 1977-86 from FSU which are based on COADS and NCDC data and objectively analysed (Legler *et al.* 1989). These pseudo-stress components are converted to stress components using a constant drag coefficient of $1.25 * 10^{-3}$ and an air density of 1.2 kg m^{-3} and considered as a forcing in the model. Since in the present study the grid resolution is 28 km, a bi-cubic spline technique is then used to interpolate the data to get the input values at the model grid points. The input wind stress and their curl for February and August are shown in Fig. 2.

We assume that the monthly mean wind data represents the value at the middle of the respective month and then linearly interpolated between two months to get the data at model time step. For simplicity model calendar is considered to be of 360 days and each month of 30 days.

3. Results and discussion

In an earlier experiment with a simple non-divergent barotropic ocean model Behera *et al.* (1992) simulated the seasonal circulation of the Arabian Sea and Bay of Bengal, while in the present study, the model geometry is extended up to 24°S, and mean monthly winds are used to force the model. Further, free surface condition and open boundary condition on open sea side are used here against the rigid lid approximation and closed boundary conditions as used in the earlier study.

In this study three experiments were carried out:

(*i*) simulation of seasonal circulation using the average monthly mean wind stress;

(*ii*) study of the inherent interannual variability because of the model physics and dynamics, when forced with the same average wind and

(*iii*) simulation of circulation and upper layer thickness using interannual wind stress as a forcing.

In the first experiment, 10-year averages of the monthly mean wind stress for the considered period used as a forcing (Fig. 2) and model was spun up from a state of rest. After 9 years of model integration, the model solutions reached a quasi steady state and results from the tenth year of integration is discussed here and is compared with the observational evidences and other model results. The model fields shown in the figures are the instantaneous snap shots of the middle of the corresponding month (mid-night of the 15th of each month which is considered as 16th day of the month). Since oceanic processes are slow the differences between monthly averages and the middle snap shots are insignificant (actually verified).

3.1. *Somali current and circulation in the Arabian Sea*

The model circulation features as seen from Fig. 3 show the major current structure in the Indian Ocean. During Northern Hemisphere winter the winds are northeasterly in the northern Indian Ocean and the Somali Current along the Somali coast flows southwestward. This is evident from the February circulation (Fig. 3a). From December to early April, these currents flow southward, flowing from 10°N to equator in December and upto 2°S during January-March. These currents are fed by onshore flow around 10°N and there is a strong offshore flow around 5°N. The southward flowing Somali Current togetherwith the northward flowing East African Coastal Current (EACC) forms an anticyclonic gyre south of equator. These model features are in qualitative agreement with the observed climatological atlases of Duing (1970), Wyrtki (1971), Hasternath & Greischar (1989), Rao *et al.* (1991) and the model results of Luther & O' Brien (1989) and Woodbery *et al.* (1989). During the transition to southwest monsoon, the surface currents along the Somali coast start flowing northward. The re-circulated water from the EACC forms a cyclonic gyre south of equator in April. This becomes stronger in May and is present throughout the monsoon season. The offshore flow south of this gyre is just around equator. From May to August, winds become stronger along the coast and coastal upwelling starts along the African coast in response to the nearshore positive wind stress curl (Fig. 2d). This is

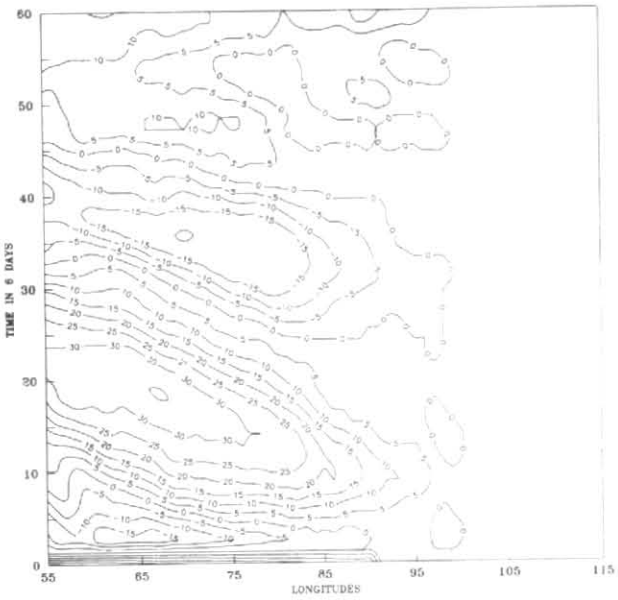

Fig. 4. Time-longitude plot along the equator of the model zonal velocity component in mean wind case. Contour interval is in 5 cm/s. The labels along the y-axis are in 6 days and start from 16 January of 10th year

inferred from the model upper layer thickness (ULT) deviation (Fig. 3d). The decrease of ULT is considered as an indicator of upwelling and *vice versa*.

An anticyclonic gyre, which is known as Great Whirl-forms around 5°N in late July and migrates northward in August (Fig. 3b). Another eddy called Socotra Eddy, east of Socotra Island forms in late July and August. These circulation features are in qualitative agreement with the observed climatological atlases and other model studies referred earlier. The formation and strengthening of the Great Whirl is often related with the negative wind stress curl which through Ekman pumping drives a geostrophic flow. The data used in the model shows a negative wind stress curl to the east of the gyre.

The circulation in the interior Arabian Sea are in Sverdrup balance flowing southward in summer and northward in winter. The circulation features and the ULT deviation along the west coast of India are in contrast to what is expected from the wind field. The generation of highs in winter (Fig. 3c) is the opposite of what would be expected from local upwelling. The change in ULT is more likely to be associated with coastal Kelvin waves generated from the wind perturbation near Sri Lanka.

3.2. *Equatorial currents*

The model-produced North Equatorial Current (NEC) flows westward in winter and eastward in summer which is more appropriately known as Monsoon Current (MC) (Figs. 3 a & b). During transition months the flow merges with the Equatorial Jet. These currents are also affected by the train of equatorial Rossby waves, restricting the eastward MC to a northern latitude during summer monsoon as against the observed broad currents near equator. This is mainly because the reported observed currents are wind driven surface currents whereas the model currents are mean upper layer flow governed by internal mode.

The model-produced Equatorial Counter Current (ECC) remains south of equator between 1°S and 7°S and is affected by the reflected equatorial Rossby waves propagating westward. The time-longitude plots of zonal velocity component along equator (Fig. 4) show clusters of wave of westward phase and eastward group propagation with a periodicity of approximately 200 days and are interpreted as Rossby waves. The coastal Kelvin wave packets also can be seen at the eastern coast. The flow is eastward in most part of the year and togetherwith the South Equatorial Current (SEC) forms the basin wide gyre in Southern Hemisphere.

The model SEC flows westward between 10°S and 20°S which is more to its north (east of 60°E) during northern summer (Fig. 3b) and is in agreement with observation. Since in this study islands and shallow banks east of Madagascar are not considered the SEC flows directly to the east coast of Madagascar and then splits, one branch flowing southward and goes out of the model domain, whereas the other branch flows northward around tip of the Madagascar. The latitude of this splitting is consistent with the observed split at 17°S (Schott *et al.* 1988) and the model results of Woodbery *et al.* (1989). The northern branch that flows around tip of Madagascar again splits at African coast, one branch flows northward and feeds the EACC and the other one flows southward as Mozambique Current.

3.3. *Circulaltion in Bay of Bengal*

The model circulaltion for the Bay of Bengal can be broadly divided into four stages. In the first stage a large basin wide anticyclonic gyre (Fig. 3a)

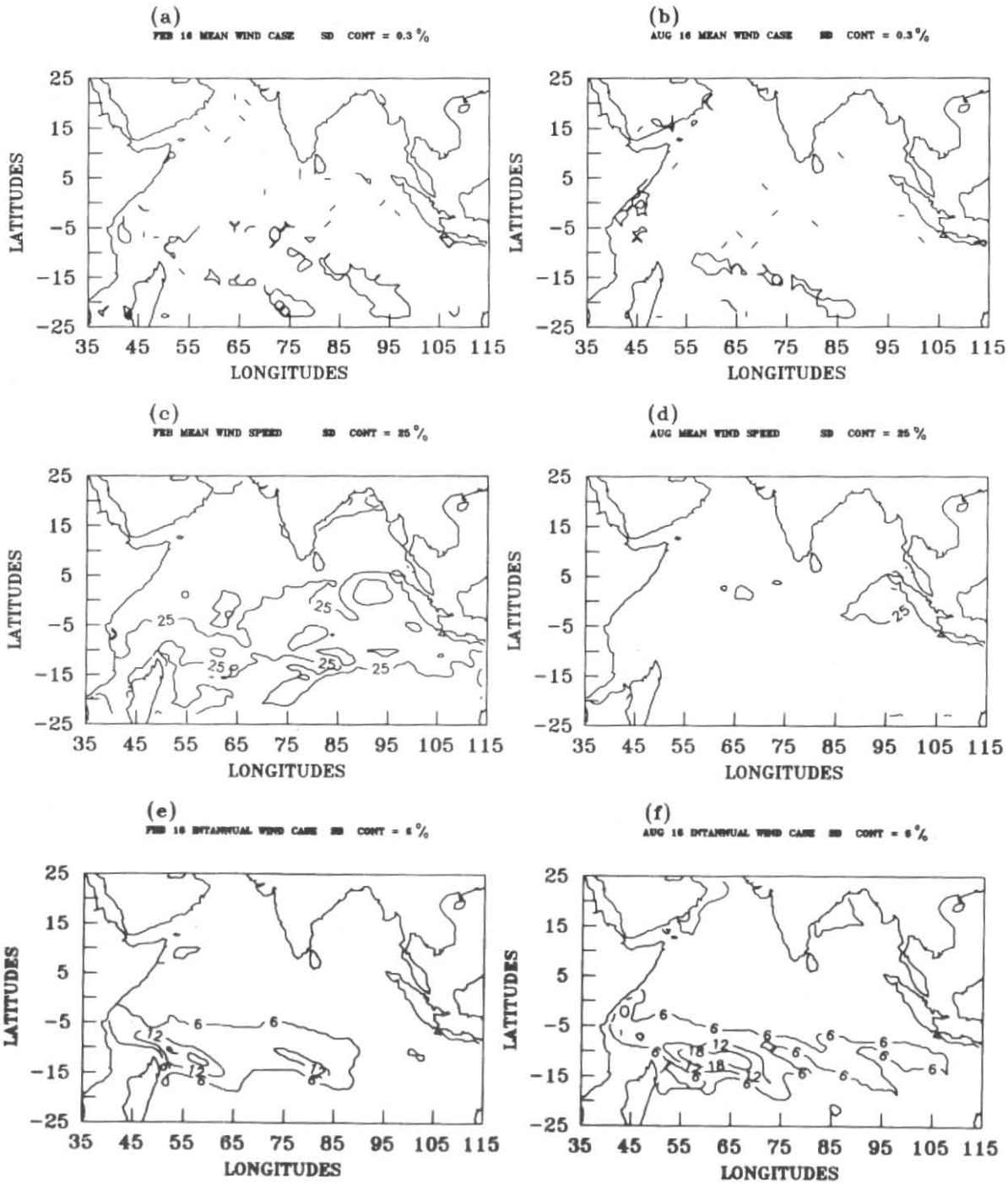

Figs. 5 (a & b). The model ULT standard deviation in percentage departure from mean from years 11th to 20th of extended model integration using same 10-year average winds; (a) 16 February, (b) 16 August. Contour interval is 0.3%; (c & d) The SD in percentage departure from mean of induced wind forcing. Contour interval is 25%; (e & f) Same as Figs. 5 (a) & (b) but in case of interannual wind. Contour interval is 6%

in winter months, *i.e.,* December-March, dominates the circulation in the Bay which is in agreement with the climatological atlases and other model studies, *e.g.,* Potemra *et al.* (1991). The gyre has a northward flow along the east coast of India north of 13°N as observed by Cutler and Swallow (1984) and inferred from satellite data by Legeckis (1987). During the transition months (April-May) the basin

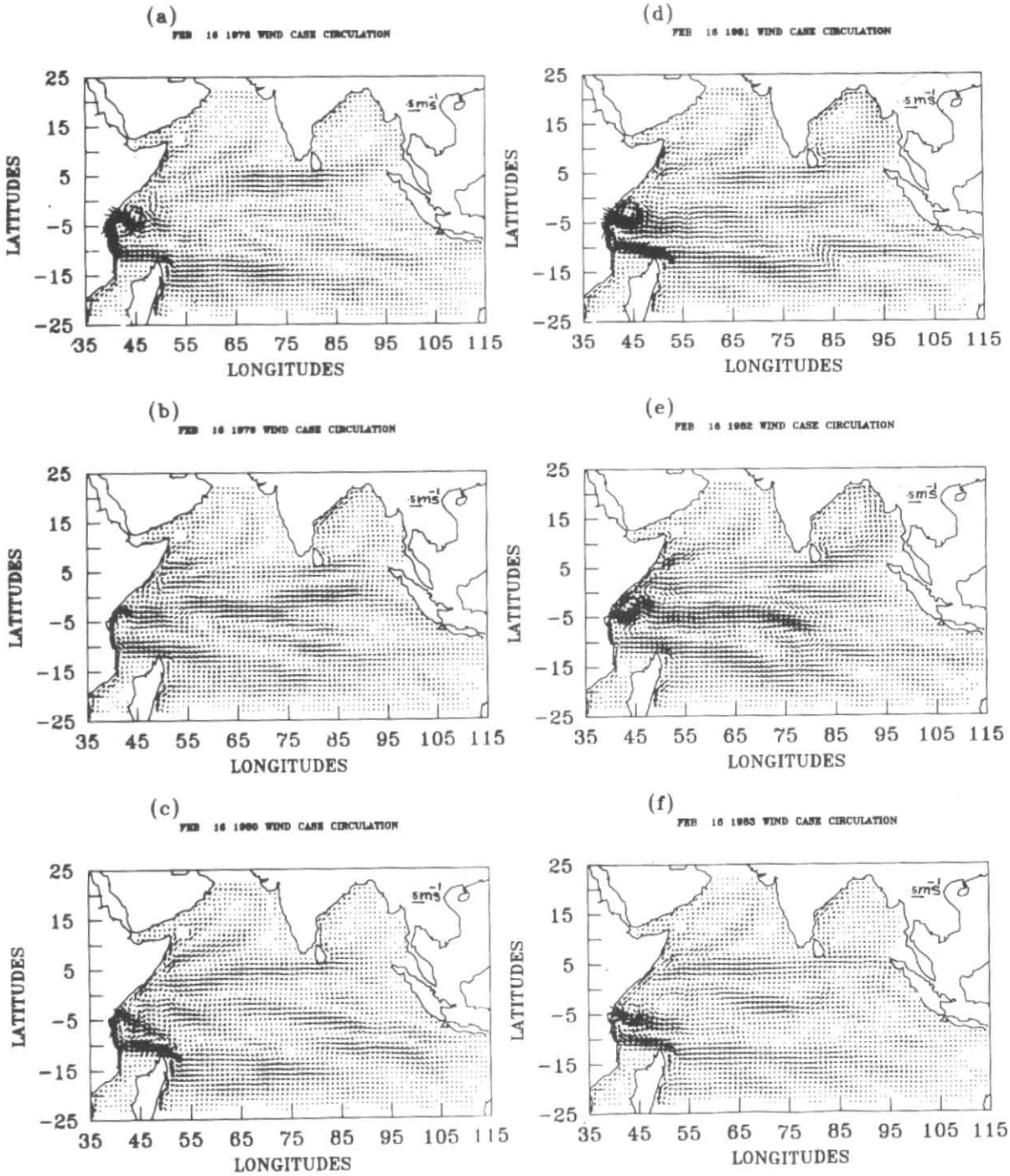

Figs. 6 (a-f). The model circulation field in case of the interannual winds for 16 February; (a) 1978, (b) 1979, (c) 1980, (d) 1981, (e) 1982 and (f) 1983

is dominated by two gyres, an anticyclonic gyre to the west and a wider cyclonic gyre to the east with northward flow along both the boundaries. During June-July the Bay is dominated by a single cyclonic gyre which is replaced again by a two gyre system during August-October (Fig. 3b, a cyclonic gyre to west and an anticyclonic gyre to the east).

3.4. *Interannual variability*

In the second experiment, the model was integrated for an extended period of 10 years, *i.e.*, from 11th to 20th year with the same wind as used in the first experiment, to study the interannual variability in the model fields. From these last

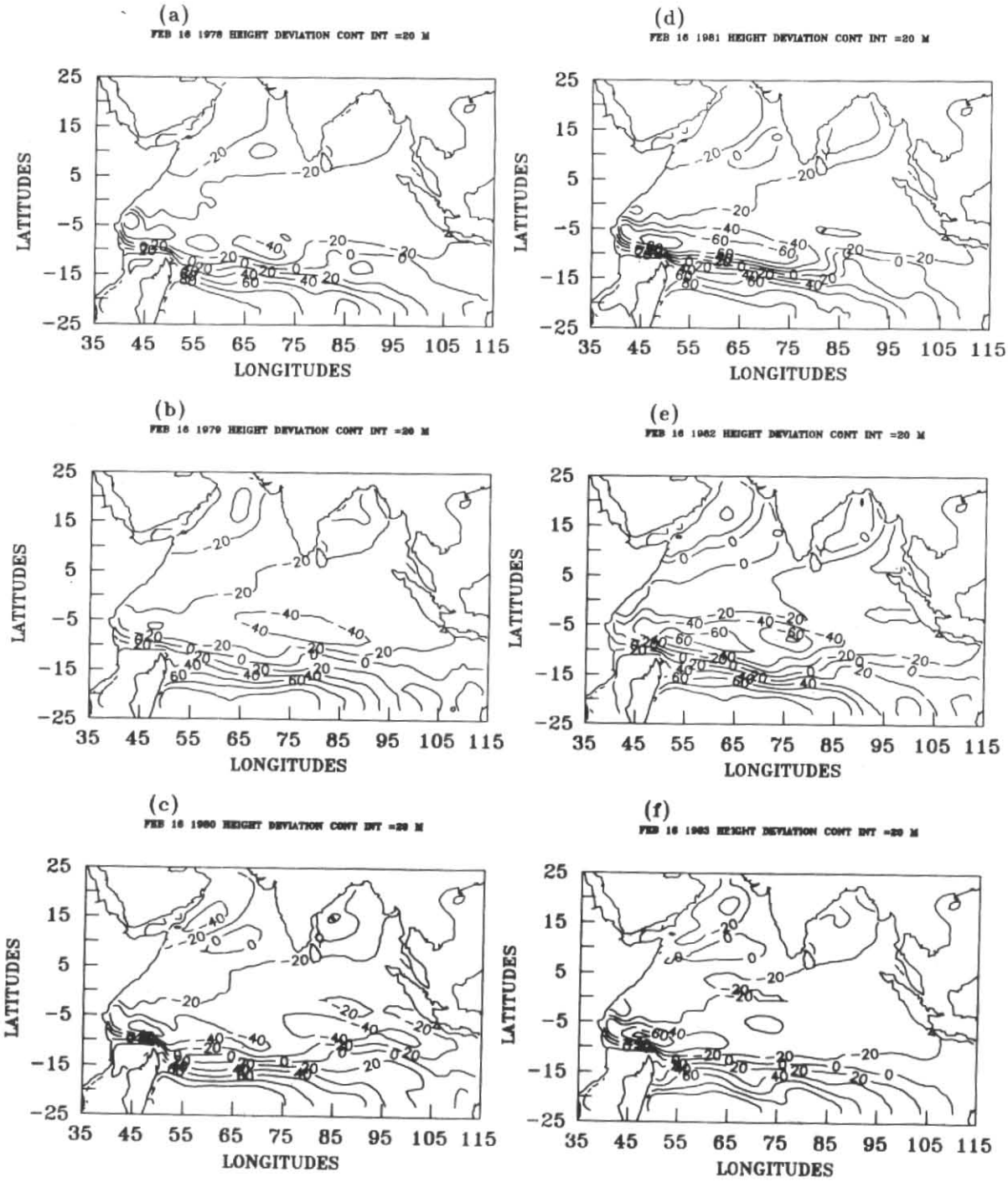

Figs. 7 (a-f). The model ULT deviation in case of interannual wind for 16 February; (a) 1978, (b) 1979, (c) 1980, (d) 1981, (e) 1982 and (f) 1983

10 years, we computed the mean and standard deviation (SD) of the model ULT field for the 16th of each month of the year at each grid point, *e.g.*, 16th January of all the years and so on. The SD fields expressed as percentage of deviation from the mean are thus an indicator of the inherent interannual variability produced by the model physics and dynamics, since the wind cycle is the same repeating from year to year. The ULT standard deviation (Figs. 5 a & b) is less than 0.6 percent from mean (1m app.) in all over the basin indicating that the model solution is a periodic response to the seasonal winds.

When the same experiment was carried out with real time interannual winds (1977-86) the model

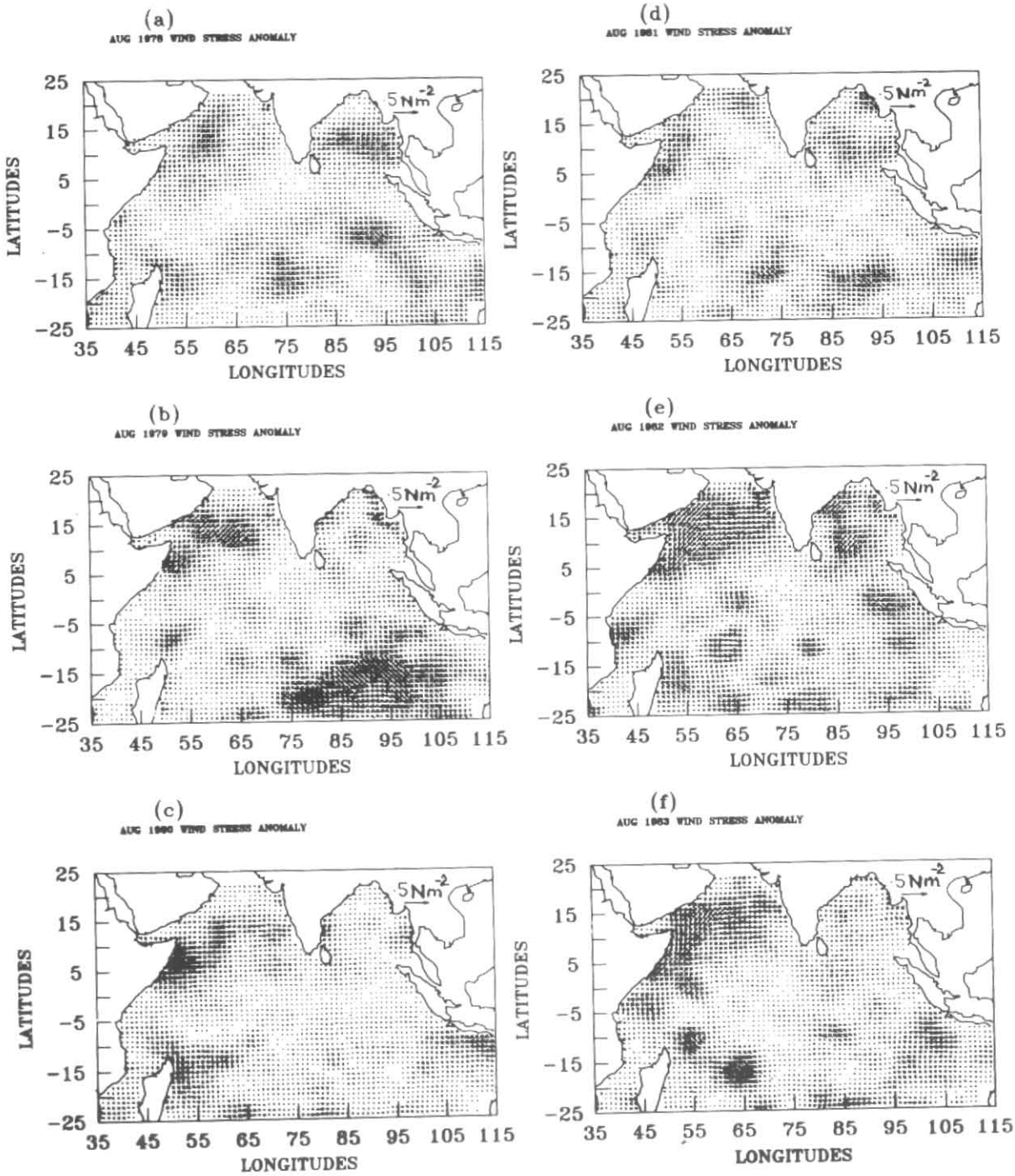

Figs. 8 (a-f). The August induced wind stress anomaly; (a) 1978, (b) 1979, (c) 1980, (d) 1981, (e) 1982 and (f) 1983

fields show larger variability. The SD of model ULT field for 16 February and 16 August, as depicted in Figs. 5 (e-f) show everywhere atleast an order of magnitude larger than the previous case, indicating that the variability in model field is solely due to the variability in wind field. The SD of the induced wind velocity magnitude (Figs. 5 c & d) for the corresponding months show higher variability in the eastern equatorial Indian Ocean which is probably because of smaller wind magnitude and larger interannual variability. But the higher variability in the model ULT field is near Madagascar coast which indicates that the variability present in the model fields are not directly forced. It seems that the variability in the model fields near Madagascar coast is because of the trapped energy from the blocking of the westward propagating Rossby waves which in turn might have been excited by the wind

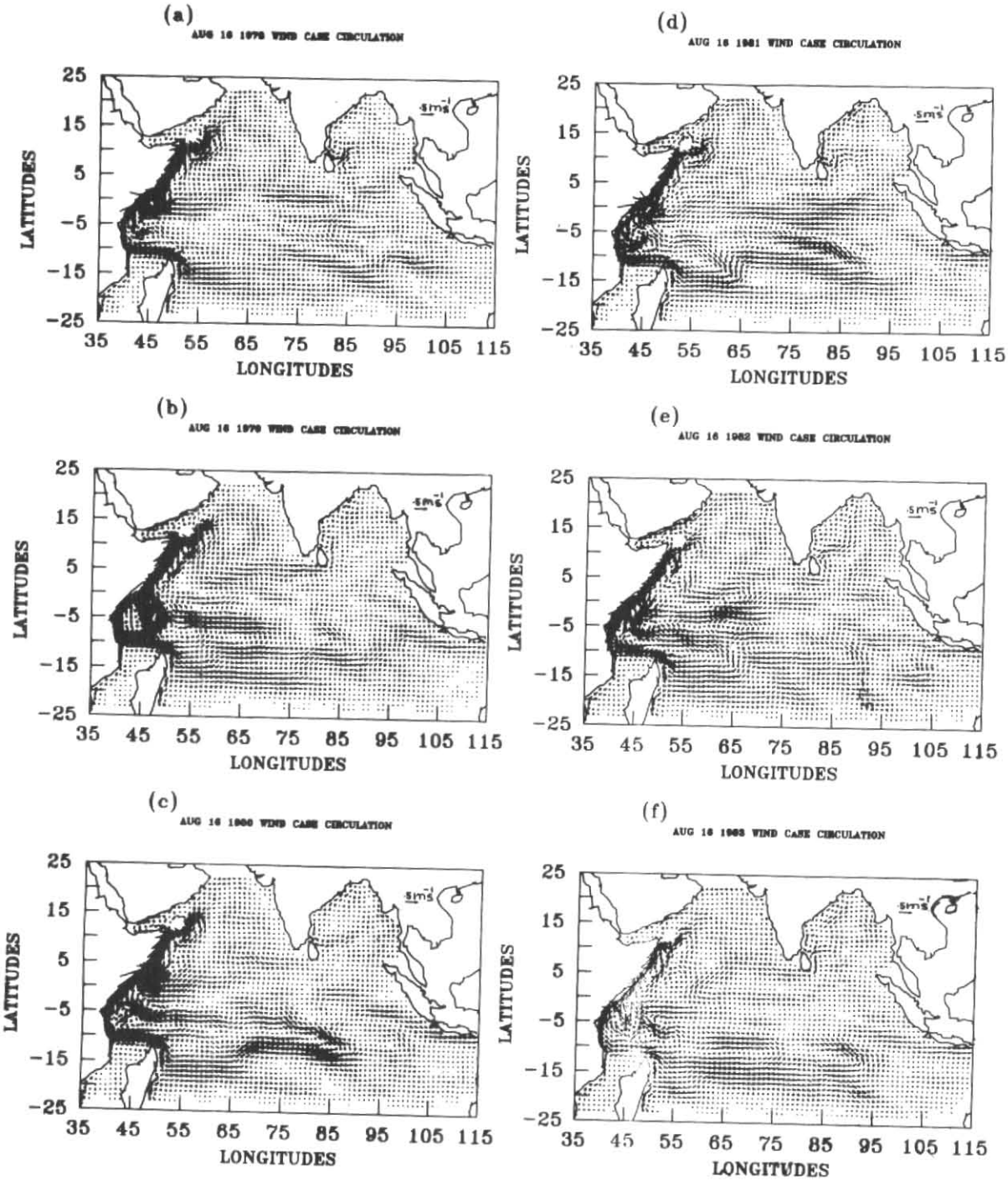

Fig. 9. Same as Fig. 6 but for August 16

variability in the region farther east of Madagascar. Variability in model fields over other regions seems also not to be directly forced. Highest and lowest variabilities are found in the months of October and May respectively. However, the months of August and February are chosen for discussion as representative months of summer and winter seasons. Further, the variability remains the same spatially, except for the intensity.

3.4.1. *A case study*

In this sub-section we will discuss the interannual variability present in model fields in the six consecutive years starting from 1978 to 1983 which include two bad monsoon years of 1979 and 1982. In general there are differences found in the model fields of all the years and wherever possible, the contrasting features found in two consecutive

contrasting monsoon years are compared with that of two normal years.

The February circulation (Fig. 6) shows variability mostly in the equatorial region and the region north of Madagascar near African coast. The ECC is found to be stronger and is covering up to 85°E in 1979 and 1982. Further, the Wyrtki Jet (Wyrtki, 1973), which generally appears in the eastern Indian Ocean in the month of April in response to the zonal wind is found as early as in February NECs in these years are restricted to a narrow band as compared to other years. The SECs north of Madagascar, flowing to the African coast found to be weaker during the two bad years and are found to be exactly repeating in the two consecutive normal years of 1980 and 1981. These variabilities are pronounced during two contrasting years as compared to two normal years. As per expectation the gradient in ULT field (Fig. 7) is maximum in the north of Madagascar in normal years that suggests a higher transport of hot water from summer hemisphere to equatorial region *via* the western boundary. The anticyclonic flow around 5°S, near the African coast is found to be present in all the years except 1979 and 1980. The model ULT deviations show maximum variability in the upwelling region (negative deviation associated with the basin wide southern hemisphere gyre), north of Madagascar. The negative deviation is maximum in 1981 and is minimum in 1979, however the deviation in 1982 is comparable with 1981. The ULT deviation also indicates a region of downwelling process in southeast Arabian Sea (hence a warmer sea), but this patch is particularly stronger in 1982 which happened to be a bad monsoon year. The higher ULT is a result of Rossby wave packets radiated from the coastal Kelvin waves of the west coast of India which in turn are radiated from Bay of Bengal. The higher ULT togetherwith the associated anticyclonic circulation are supported by a recent study of Bruce *et al.* (1994).

We then turn to the variability present in the height of summer monsoon in response to anomalous wind (Fig. 8) as shown in August circulation (Fig. 9). The two-gyre system (Southern Gyre and Great Whirl) is found in all the years. A northward migration of the Southern Gyre can be seen in the model circulation fields of 1980. In other years, eddies from the Southern Gyre move northward to merge with the Great Whirl as reported in observational studies and other modelling studies (Swallow and Fieux 1982 and Luther *et al.* 1985). The August circulation fields show maximum variability in the recirculation region of the EACC (between equator and 10°S off Africa Coast) as a result of formation of eddies east of this region and being reabsorbed into the EACC. The formation of these eddies seems to be in response to anomalous wind north of Madagascar (Fig. 8) that generates westward propagating Rossby waves. In 1979 case, the recirculation of the EACC has turned into such an eddy disturbing the shape of Southern Gyre. The position and intensity of these eddies vary from year-to-year in response to the changes in wind forcing. The basin wide gyre of the Southern Hemisphere is near identical in two consecutive normal years of 1980 and 1981 as compared to other years as a result of less variability in wind stress curl of the region. In the equatorial region, MCs are restricted to the tip of Indian peninsula in all the years except for the 1978 case where these currents are found near equator. Further, in the 1981 case a strong westward current is found over the equatorial region, inspite of the fact that both 1978 and 1981 had less variability in the wind forcing over the region (Fig. 8). However, in both cases there are anomalous zonal winds found in the central and the eastern equatorial region during the previous couple of months suggesting that the changes are in response to the reflected Rossby waves generated by anomalous wind. There are less variability found in the Arabian Sea circulation, although the forcing has a greater variability over the region (Fig. 8) suggesting that the circulation over the region is highly consistent seasonal cycle and is not affected much by the changes in wind forcing. The flow along the Yemen and Oman coast shows interannual variability, being stronger in the years having stronger wind and is particularly very strong in 1982 in response to the strong anomalous wind.

In the Bay of Bengal, the cyclonic eddy off the coast of Madras is weaker in bad monsoon years as well as in the good monsoon year 1980. Further, although the winds in 1982 were anomalously stronger over the region, the eddy is almost absent indicating the influence of reflected downwelling Rossby waves (at different phase of the westward spreading of the northward flow found at the center of the Bay) from Burma Coast in the circulation of the Bay. The phase and amplitude of these

waves give rise to the variability. There are no similarity in the circulation field of the Bay during two consecutive normal years.

4. Conclusion

The model has simulated realistically most of the observed general circulation features of the Indian Ocean when forced with a repeating seasonal cycle of wind. The formation of Somali Currents and the associated gyres over time and space are realistic. The four stages in the circulation pattern of the Bay of Bengal as reported by other model studies is observed in the model fields. The summer circulation of the Bay of Bengal seems to be in response to the remote forcing from equatorial Indian Ocean through the downwelling reflected Rossby waves from the coastal Kelvin waves propagating along the eastern boundary.

In an extended integration for ten years with the same ten-year averaged wind, model fields do not show any spurious interannual variability because of model physics and dynamics. When forced with interannual wind, every year shows general differences from the other years and there are less similarities found in the model fields even during two consecutive normal years. Reasoning for such variability is beyond the scope of the present paper. The variability in induced forcings and the model outputs show less direct relationship. In general, the ECC in February is found to be stronger in bad monsoon years. Further the flow field and the ULT deviation field indicate a stronger westward flow north of Madagascar in good monsoon years suggesting a higher transport of hot water to the equatorial region from the southern hemisphere. This particular aspect is being investigated in detail for a possible link between model ULT deviation in subsequent months and the Indian summer monsoon rainfall. The northward migration of the Southern Gyre during August is found in the year 1980. In all other years eddies from Southern Gyre move northward to merge with the Great Whirl. The basin wide gyre of the Southern Hemisphere shows less variability in August during two consecutive normal years. However, circulation in the Arabian Sea does not show much interannual variability, suggesting a consistent seasonal cycle irrespective of wind forcing. The interannual variability in the model fields of the Bay of Bengal are dependent on the phase and amplitude of the reflected Rossby waves from Burma coast. The model is now being modified to include more active layers so that the undercurrents can be simulated and also such a model allows the vertical propagation of kinetic energy. The thermo-dynamic effect is also being included in the model as in McCreary *et al.* (1993) to simulate the interannual SST field.

Acknowledgements

We are thankful to the Director, Indian Institute of Tropical Meteorology for his interest in the work. We are indebted to Prof. J. J. O' Brien, Dr. M. E. Luther and Dr. J. N. Stricherz for graciously supplying the wind data and all the helpful suggestions. We are grateful to the referee for going through the paper in detail and providing a scope for improvement. We are thankful to Mr. V. R. Mujumdar for allowing us to use his graphics software. The computations were carried out in the HP 9000/735 workstation at the Institute.

References

Behera, S. K., Sawant, H. J. and Salvekar, P. S., 1992, "Simulation of north Indian Ocean circulation using a simple barotropic model and some sensitivity studies", *Mausam*, **43**, 353-360.

Bruce, G. J., Donald, R. J. and Kindle, C. J., 1994, "Evidence for eddy formation in the eastern Arabian Sea during the northeast monsoon", *J. Geophys. Res.*, **94**, C4, 7651-7664.

Cadet, D. L. and Diehl, B. C., 1984, "Interannual variability of surface fields over the Indian Ocean in recent decades", *Mon. Weath. Rev.*, **112**, 1921-1985.

Camerlengo, A. L. and O' Brien, J. J., 1980, "Open boundary conditions in rotating fluid", *J. Comp. Phys.*, **35**, 12-35.

Cox, M. D., 1970, "A mathematical model of the Indian Ocean," *Deep Sea Res.*, **17**, 47-75.

Cutler A. N. and Swallow, J. C., 1984, Surface currents in the Indian Ocean; compiled from historical data archived by the Meteorological Office, Bracknell, UK, Rep., 187, 8 p.

Das, P. K., Dube, S. K., and Rao, G. S., 1987, "A steady state model of the Somali Current", Proc. Indian Acad. Sci., 96, 279-290.

Dube, S. K., Luther, M. E. and O' Brien, J. J., 1990, "Relationships between interannual variability in the Arabian Sea and Indian monsoon rainfall", *Meteor. Atm. Phys.*, **44**, 153-165.

Duing, W., 1970, The monsoon regime of the currents in the Indian Ocean, East-West Center Press, Honolulu, 68 p.

Gill, A. E., 1980, "Some simple solutions for heat induced tropical circulations", *Quart. J. R. Met. Soc.*, **106**, 447-462.

Hasternath, S. and Greischar, L. L., 1989, Climate atlas of the Indian Ocean, Part-III, Upper ocean structure. The University of Wisconsin Press, 247 charts.

Jensen, R. G., 1990, A numerical study of the seasonal variability of the Somali Current, Ph. D. dissertation, Florida State Univ., 118 p.

Legeckis, R., 1987, "Satellite observations of a western boundary current in the Bay of Bengal", *J. Geophys. Res.*, **92**, 12, 974-12, 978.

Legler, D. M., Navon, J. M. and O' Brien, J. J., 1989, "Objective analysis of pseudostress over the Indian Ocean using a direct minimisation approach", *Mon. Weath. Rev.*, **117**, 709-720.

Luther, M. E., O' Brien, J. J. and Meng, A. H., 1985, Morphology of the Somali Current system during the southwest monsoon; Coupled ocean-atmosphere models, Ed. J. C. J. Nihoul, Elsevier Science Publ.

Luther, M. E. and O' Brien, J. J., 1989, Modelling the variability in Somali Current, Meso scale/Synoptic coherent structure in Geophysical turbulence, Eds. J. C. J. Nihoul and B. M. Jamart, Elsevier Science Publ. 373-386.

McCreary, P. J. and Kundu, P. K., 1988, "A numerical investigation of the Somali Current during the Southwest Monsoon," *J. Mar. Res.*, **46**, 25-58.

McCreary, P. J., Kundu, P. K., and Molinari, R. L., 1993, "A numerical investigation of dynamics, thermodynamics and mixed layer processes in the Indian Ocean", *Prog. Ocean.*, **31**, 181-244.

Potemra, J. J., Luther, M. E. and O' Brien, J. J., 1991, "Relationships between interannual variability in the Arabian Sea and Indian monsoon rainfall", *J. Geophys. Res.*, **96**, 12, 667-12, 683.

Rao, R. R., Molinari, R. L., Festa, J. F., 1991, Surface meteorological and near surface oceanographic atlas of the tropical Indian Ocean, NOAA Technical Memorandum, ERL AOML-69.

Schott, F., Fieux, M., Kindle, J., Swallow, J. and Zantopp, R., 1988, "The boundary currents east and north of Madagascar, Direct measurements and model comparison," *J. Geophys. Res.*, **93**, 4963-4974.

Swallow, J. C. and Fieux, M., 1982, "Historical evidence for two gyres in the Somali Current", *J. Mar. Res.*, **40**, 747-755.

Woodberry, K. E., Luther, M. E. and O' Brien, J. J., 1989, "The wind driven seasonal circulation in the southern tropical Indian Ocean", *J. Geophys. Res.*, **94**, 17, 985-18, 002.

Wyrtki, K., 1971, Oceanographic atlas of the International Indian Ocean Expedition, National Science Foundation, Washington, D. C. 531 p.

Wyrtki, K., 1973, "An equatorial jet in the Indian Ocean", *Science*, **181**, 262-264.

Zebiac, S. E. and Cane, M. A. 1987, "A model ENSO", *Mon. Weath. Rev.* **115**, 2262-2278.